

Joint Source and Turbo Trellis Coded Hierarchical Modulation for Context-aware Medical Image Transmission

Abdulah Jeza Aljohani, Hua Sun, Soon Xin Ng and Lajos Hanzo

School of Electronics and Computer Science, University of Southampton, SO17 1BJ, United Kingdom.

Tel: +44-23-8059 3125, Fax: +44-23-8059 4508

Email: {ajra1c09,hs4g09,sxn,lh}@ecs.soton.ac.uk, <http://www-mobile.ecs.soton.ac.uk>

Abstract—An iterative Joint Source and Turbo Trellis Coded Hierarchical Modulation is introduced for robust context-aware medical image transmission. Lossless source compression as well as Quality of Service (QoS) might be considered as the main constraints in the telemedicine field. Our proposed scheme advocated was design to exploit both the joint source-and-channel iterative decoding and the cooperative structure in order for tackling these requirements. The Source Node (SN) is constituted by a lossless Variable Length Code (VLC) and Turbo Trellis-Coded Modulation (TTCM) which relies on Hierarchical Modulation (HM). The Relay Node (RN) is used to support the transmission of the most important content of the image. Our proposed scheme exhibits a robustness performance over a realistic uncorrelated Rayleigh fading channel, while it outperforms the non-cooperative scheme by 3 dB at asymptotic (error-free) Peak Signal to Noise Ratio (PSNR) value.

Index Terms—Hierarchical Modulation, joint source channel coding, m-health, Turbo Trellis Coded Modulation, wireless telemedicine.

I. INTRODUCTION

Recent development in wireless communications as well as in telemedicine-aided devices has led to a rapid improvement in the delivery of the healthcare services. A new paradigm of Mobile healthcare (m-health) has emerged in which healthcare services could be provided at any time and any where [1], [2]. Two main issues, however, could affect the deployment of such systems [1]. Firstly, a large data volumes is associated with medical multimedia data, hence a bandwidth-efficient schemes would be required [3]. A cardiac ultrasound loops of 30 seconds, for example, needs a 196 M Bytes [4] of bandwidth. The second issue is that, lossless compression techniques are often required in telemedical applications in order to avoid the loss of information which might be vital for the diagnosis. Several practical applications have been proposed to overcome the aforementioned concerns. Context-aware ultrasonography based video transmission over WiMAX scheme, was proposed in [4], while an adaptive scalable image and video compression based different wireless medical network is proposed in [3].

Trellis Coded Modulation (TCM) and Turbo TCM (TTCM) are bandwidth efficient schemes that integrated the coding and modulation functions in a single block. TTCM [5] has a structure similar to that of the family of binary turbo codes, where two identical parallel-concatenated TCM schemes are employed as component codes. The classic TTCM design was outlined in [5], based on the search for the best TCM component codes using the so-called ‘punctured’ minimal distance criterion, in order to approach the capacity of the Additive White Gaussian Noise (AWGN) channel. Recently, various improved TTCM schemes were designed in [6] with the aid of Extrinsic Information Transfer (EXIT) charts and union bounds for approaching the capacity of the Rayleigh fading channel.

The financial support of the Saudi Ministry of Higher Education and that of the European Union’s Seventh Framework Programme (FP7/2007-2013) under the auspices of the CONCERTO project (grant agreement no 288502) of the RC-UK’s India-UK Advanced Technology Centre (IU-ATC) as well as of the European Research Council’s Advanced Fellow grant is greatly appreciated.

Hierarchical Modulation (HM), also known as layered modulation, has been considered as an efficient solution for maintaining the Quality of Service (QoS) for the increasing number of the wireless networks subscriber [7]. The main feature of HM is the capability of manipulating multiple simultaneous data streams by modulating them onto a number of different layers with different protection levels according to their priorities, where each of the different layers may be demodulated separately [7]. That is to say HM multiplexes layers of different robustness into one stream. The HM scheme has been investigated by Alouini in [8], [9] in terms of the general mapping model, complexity analysis and BER performance. HM scheme has also been incorporated in cooperative communication systems in [9]–[11].

Joint Source and Channel Coding/Decoding (JSCC/D) techniques have been designed for limited-delay, limited-complexity video systems communicating over wireless channels because in this practical scenario, Shannon’s source and channel coding separation theorem [12] has a limited validity. JSCC/D schemes are typically constituted of serially-concatenated iterative decoders, aiming for exploiting the unintentional residual redundancy of the source and the intentionally imposed redundancy of the channel codes [13]. Recently, Joint Source/Channel Coding and Modulation (JSCM) schemes were studied in [13], which were further extended to a cooperative scenario in [14], [15].

Against this background, in this treatise we employ different state of the art communication techniques to enhance the multimedia telemedicine wireless transmission. We use only a medical image in this paper, although the scheme could invoke video transmission with some further considerations. An iterative joint Turbo Trellis Coded HM (TTCHM) with a lossless Variable Length Code (VLC) decoding (TTCHM-VLC) scheme for cooperative communications in a Rayleigh fading channel is proposed for medical images scenarios. Furthermore, a context awareness approach is invoked in order to improve the quality of the Region of Interest (ROI) by transmitting it via the Relay Node (RN) for attaining cooperative relaying gain. Hence, this region will enjoy the cooperative gain link, while the Region of Non Interest (RONI) will be transmitted directly to the Destination Node (DN). In a nutshell, we propose a novel end-to-end scheme that would improve the robustness of the wireless communications by invoking the iterative joint decoding scheme of [15] while enhancing the bandwidth efficiency by employing a high-order TTCHM as in [11].

The rest of the paper is organized as follows. The system model is described in Section II. Furthermore, the analysis of the proposed scheme is provided in Section II-C and its performance is evaluated in Section III. Finally, our conclusions are offered in Section IV.

II. SYSTEM DESCRIPTION

A. System Model

We consider the cooperative Decode-And-Forward (DAF) scheme of Fig. 1. In the first time slot transmission, namely Phase-I, the Source Node (SN) will either broadcast its signal $\{x_1\}$ to both RN and DN or only transmit them directly to DN, according to the image priority context. Then the RN decodes the stream $\{x_1\}$ to produce the re-encoded stream $\{x_2\}$, which would be forwarded to the DN during the second time slot, namely Phase-II. Next, the DN will recover $\{x_1\}$ based either on the pair of frames received from the SN and RN or based on the direct link of the SN.

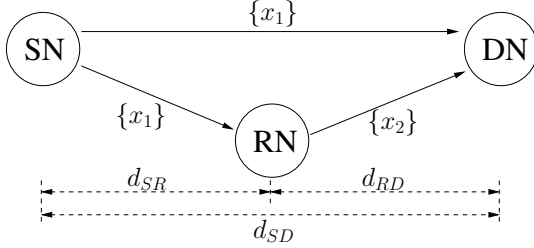


Fig. 1: Schematic of a single-relay cooperative system, where d_{SD} is the geographical distance between Source Node (SN) and Destination Node (DN).

The communication links shown in Fig 1 are subjected to an uncorrelated Rayleigh flat-fading channel, where both receivers were assumed to have a perfect Channel State Information (CSI) knowledge. The received signal at the DN during Phase-I can be written as:

$$y_{SD} = \sqrt{G_{SD}}h_{SD}x_1 + n_{SD}, \quad (1)$$

while the symbol received by the RN is:

$$y_{SR} = \sqrt{G_{SR}}h_{SR}x_1 + n_{SR}, \quad (2)$$

where the subscripts SD and SR represent the SN-DN and SN-RN links, respectively. While the received signal at the DN during the Phase-II which is transmitted from the RN, may be expressed as:

$$y_{RD} = \sqrt{G_{RD}}h_{RD}x_2 + n_{RD}, \quad (3)$$

where the subscript RD represents the RN-DN link. Additionally, the notations h_{SD} , h_{SR} and h_{RD} denote the complex-valued coefficients of the uncorrelated Rayleigh fading for the different links, while n_{SD} , n_{SR} and n_{RD} denote the Additive White Gaussian Noise (AWGN) having a variance of $N_0/2$ per dimension. Assuming a free-space path-loss model, the corresponding Reduced-Distance-Related Path-Loss Reduction (RDRPLR) factor experienced by both SR and RD links with respect to the RN and SD link as a benefit of its reduced distance and path-loss, can be calculated, respectively, as [15], [16]:

$$G_{SR} = \left(\frac{d_{SD}}{d_{SR}}\right)^2 = 4; \quad G_{RD} = \left(\frac{d_{SD}}{d_{RD}}\right)^2 = 4. \quad (4)$$

B. Region of Interest and Hierarchical Modulation

It is well known that, medical multimedia images and video sequences usually contain an important area that is vital for the diagnosis and a background area which is not that critical [3]. Hence, ROI coding appears to be an attractive solution to improve the quality of the critical area, in which more resources will be devoted to that area [4]. The definition of a ROI area can be performed automatically or by the clinician¹. In our work, and for the aim of context-aware

¹In this paper we will not discuss the ROI separation techniques in details, further information can be found in [4] and the references therein.

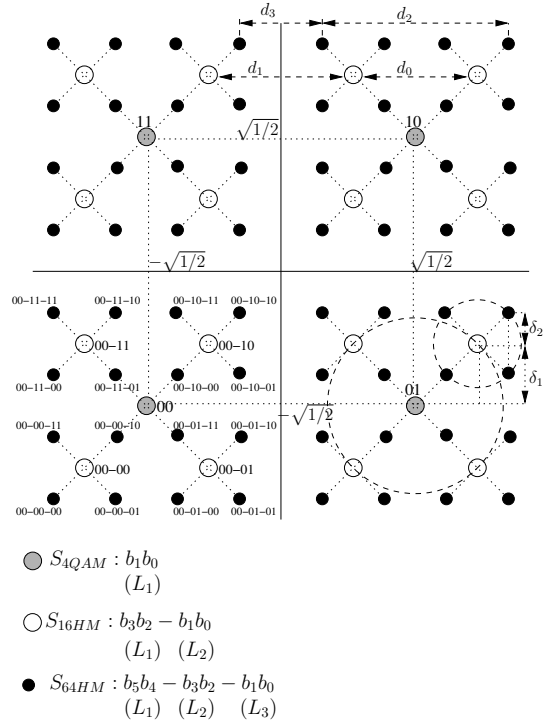


Fig. 2: The constellation diagram of the HM scheme.

design we identify ROI as the area inside the non-regular grey shape, while the RONI as the black background as illustrated in the MRI image of Fig. 6a.

The constellation diagram of a typical 64-ary HM set (S_{64HM}) is portrayed in Fig. 2. Typically, the coded symbols will be partitioned into different layers in which every two bits will be mapped to a single layer. Similar to the conventional HM scheme, we partition the coded symbols into different layers and map two data bits to each layer. Moreover, we utilise the optimised bit-to-symbol mapping technique of [11], alongside with Set-Partitioning (SP) technique, in order to reduce the overall Symbol Error Ratio (SER). The SP scheme would assign the parity bit to the least protected constellation-position. As illustrated in Fig. 2, the coded symbols would be partitioned into different layers and map two data bits to each layer. With the aid of Fig. 2, the two most significant bits (MSBs) are mapped to the base layer, where their constellation points can be considered as the 4QAM set ' S_{4QAM} ', which are shown by the four grey-shaded circles in Fig. 2. Then, the second layer, or the twin-layer, of the 16-ary HM set S_{16HM} is generated from the base layer as [11]:

$$S_{16HM} = \alpha \left[S_{4QAM} \pm \sqrt{2}\delta_1 e^{\pm \frac{\pi}{4}j} \right], \quad (5)$$

where the parameters δ can be used to define the normalization factor $\alpha = 1/\sqrt{1+2\delta_1^2}$ which maintains the average power of the constellation at unity. For the sake of simplicity we define $R_1 = d_1/d_0$ where d_0 and d_1 are the distances as shown in Fig. 2, hence, δ_1 is related to R_1 as [11]:

$$\delta_1 = \frac{d_0}{\sqrt{2}\sqrt{2}} = \frac{d_0}{\sqrt{2}(d_0 + d_1)} = \frac{1}{\sqrt{2}(1 + R_1)}, \quad (6)$$

where R_1 is in the range $0 < R_1 < \infty$. From Eq. (5) and Eq. (6) and as it is shown in Fig. 2, changing the value of R_1 would change the constellation diagram pattern. Similar procedure can be used for generating the S_{64HM} .

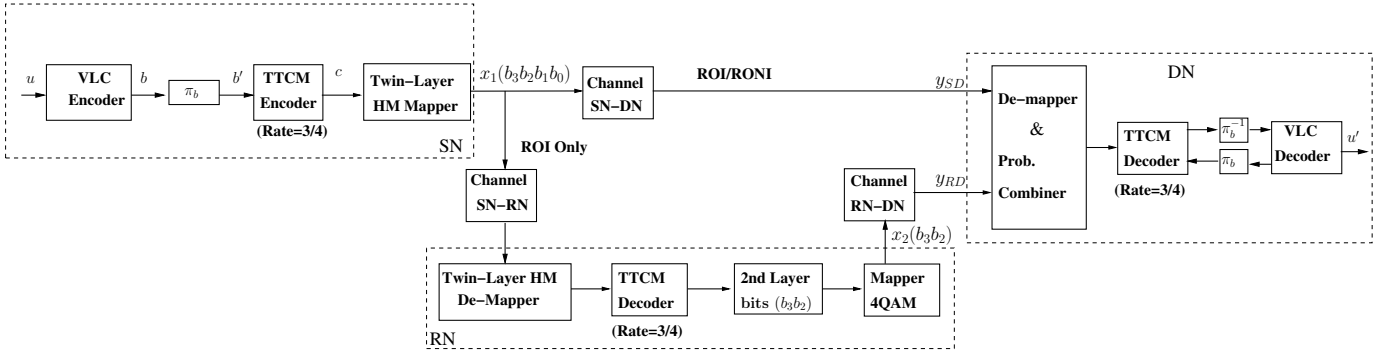


Fig. 3: The schematic of the proposed TTCHM-VLC assisted image transmission for telemedicine. Here MRI image of Fig. 6a has been used, where the ROI would enjoy the relaying path, while RONI is transmitted directly to the DN.

C. System Structure

The block diagram of the proposed TTCHM-VLC aided cooperative communication for image transmission is shown in Fig. 3, where the twin-layer 16-ary HM (16HM) is used. We opt for this arrangement, since TTCM-VLC was found to be the best one from a range of other coded modulation assisted VLC schemes in [17]. We assume that, the ROI area is selected by a medical specialist and extracted prior to the transmission. The SN employs a serial concatenated Reversible VLC (RVLC)² and a TTCHM scheme. A bit interleaver is invoked between the VLC and the TTCM, in order to enhance the iterative decoding at the receiver.

To elaborate more, we use the lossless trellis-based RVLC proposed in [20] to compress the source output stream $\{u\}$. Prior to the VLC encoder, we invoke the first method (M1) explained in Sec. V of [15] in which the image pixels will be represented by a reduced number of codewords. Each 8 bits-per-pixel (p/b) symbol of the image would be, simply, split into two 4 b/p symbols, which reduces the number of possible symbols from $2^8 = 256$ to $2^4 = 16$. The total number of source symbols of the MRI image would be increased from $512 \times 512 = 262144$ to 524288 . However, the number of the VLC trellis states will be reduced dramatically from 965 to 30. Thus, this method will reduce the complexity of the VLC decoding significantly.

The interleaved VLC-coded bit sequence $\{b'\}$ is encoded by the 16QAM-based TTCM encoder. Then, the HM scheme divides the 16QAM symbol into two layers of two bits each. The bits in the codewords of the 16HM symbol are denoted as $b_3b_2 - b_1b_0$, where b_1b_0 lay in the base layer L_2 while b_3b_2 occupy the second layer L_1 . The two information bits in L_2 decide which particular quadrant the transmitted symbol comes from and the two bits contained in L_1 identify the exact location of the transmitted symbol in each quadrant, as illustrated in Fig. 2. We use an MRI image of size (512×512) -pixel, where the image is encoded row-by-row from the top-left corner to the bottom-right corner. Each row will be divided into 4 frames, hence each frame has a size of 128 8-bit-size pixels which would increase to 256 4-bit-size pixels after applying pixel splitting method M1. Then, if the encoded frame, F_i , does not lie in the ROI, the SN will transmit the VLC-TTCHM coded symbols $\{x_1\}$ directly to the DN as 16HM signals. A single flag bit, R_i will be added to F_i indicating whether the encoded frame belongs to ROI or not. We assume that the R_i is perfectly decoded. Then the DN will demap both layers, namely L_1 and L_2 in the received y_{SD} . The probability of detecting L_1 and L_2 when y_{SD} is received at the DN

²Our design is applicable to any VLCs. However, the reversible VLCs are particularly suitable for iterative detection, because they have a minimum free distance of 2, as detailed in [18] and [19]. This allows the iterative detector to approach a vanishingly low BER at low SNR.

can be expressed as:

$$P(L_1^{(i)}, L_2^{(i)} | y_{SD}) = \frac{1}{\sqrt{2N_0}} \exp \left(-\frac{|y_{SD} - \sqrt{G_{SD}} h_{SD} S_{16HM}^{(i)}|^2}{N_0} \right) \quad (7)$$

However, the cooperative relaying will be invoked if the encoded frame lies in ROI. The VLC-TTCHM coded symbols $\{x_1\}$ will be broadcast to both the RN and DN in Phase-I. The DN in this time slot will demap $\{x_1\}$ as a 4QAM symbol aiming for recovering the two MSBs, of higher error resilience, information contained in L_1 . The probability of detecting L_1 at DN, when y_{SD} was received may be expressed as:

$$P(L_1^{(i)} | y_{SD}) = \frac{1}{\sqrt{2N_0}} \exp \left(-\frac{|y_{SD} - \sqrt{G_{SD}} h_{SD} S_{4QAM}^{(i)}|^2}{N_0} \right) \quad (8)$$

The RN, however, is capable of decoding the entire frame $\{x_1\}$ from the SN for detecting $L_1(b_3b_2)$ and $L_2(b_1b_0)$. Then, only the LSB pair in $L_2(b_1b_0)$ is mapped to the general 4QAM symbols for transmission to the DN within the frame $\{x_2\}$, during Phase-II. DN will demap $\{x_2\}$ from RN by computing the probability of receiving L_2 , when y_{RD} was received:

$$P(L_2^{(j)} | y_{RD}) = \frac{1}{\sqrt{2N_0}} \exp \left(-\frac{|y_{RD} - \sqrt{G_{RD}} h_{RD} S_{4QAM}^{(j)}|^2}{N_0} \right) \quad (9)$$

where $j \in \{0, 1, 2, 3\}$.

Finally at the DN, the probability of the 16HM symbols x_1 and x_2 is estimated using:

$$P(L_1^{(i)}, L_2^{(j)} | x_1) = P(L_1^{(i)} | y_{SD}) \cdot P(L_2^{(j)} | y_{RD}) \quad (10)$$

where $i, j \in \{0, 1, 2, 3\}$. Our context-aware based cooperative transmission can be summarised as follows:

if $F_i \subset \text{ROI}$; then

Phase-I

SN broadcasts $L_1(b_3b_2)$ and $L_2(b_1b_0)$

RN demaps $L_1(b_3b_2)$ and $L_2(b_1b_0)$

DN demaps $L_1(b_3b_2)$

Phase-II

RN decode-and-forward $L_2(b_1b_0) \rightarrow \text{RN}$

DN demaps $L_2(b_1b_0)$

else

Phase-I

SN broadcasts $L_1(b_3b_2)$ and $L_2(b_1b_0) \rightarrow \text{DN}$

DN demaps $L_1(b_3b_2)$ and $L_2(b_1b_0)$

end if

Note that the DN would demap the signals x_1 and x_2 as two 4QAM symbols if $F_i \subset \text{ROI}$, but the number of modulation levels in the TTCHM decoding block of Fig. 3 is 16. Explicitly, we employ a rate-3/4 convolutional code as the constituent code of the TTCM [5]. The constraint length was chosen to be $k = 3$ and the generator polynomials (octal format) are $H(D) = [11\ 02\ 04\ 10]$. In our forthcoming investigations, we will adapt the parameter R_1 for optimizing the performance of the system. Finally, the received information sequence $\{u'\}$ is estimated by exchanging *extrinsic* information between the TTCM and VLC decoders, as shown in Fig. 3.

III. PERFORMANCE EVALUATION

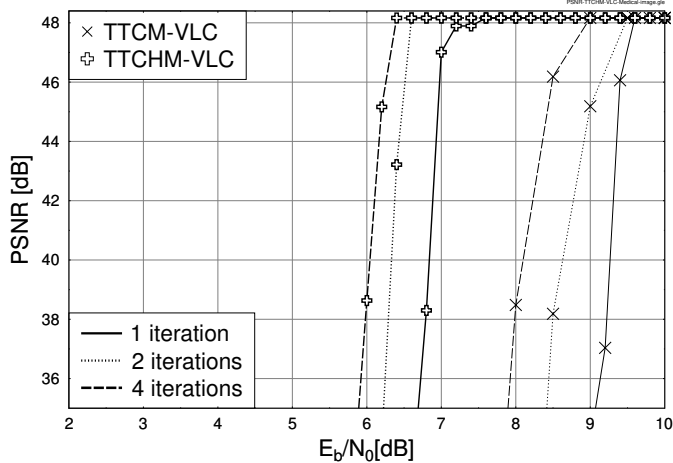


Fig. 4: The PSNR versus E_b/N_0 performance of 16HM-based TTCHM-VLC scheme for cooperative communication system when communicating over uncorrelated Rayleigh fading channel, where the $R_1 = 1.6$.

The classic Peak Signal-to-Noise Ratio (PSNR) as well as the subjective image quality were used to examine the performance of the proposed scheme, where PSNR for an $(m \times n)$ -pixel monochrome can be calculated as:

$$PSNR = 10 \log_{10} \left(\frac{I_{\max}^2}{\frac{1}{mn} \sum_{i=0}^{m-1} \sum_{j=0}^{n-1} |I_{i,j} - \hat{I}_{i,j}|^2} \right), \quad (11)$$

where we have $m = n = 512$ in our image, while $I_{i,j}$ and $\hat{I}_{i,j}$ here denote the original image pixel and the estimated pixel of the decoded image, respectively. The I_{\max}^2 represents the maximum possible pixel of the image, here in our simulation we have $I_{\max}^2 = 2^8 - 1 = 255$. As the employed VLC is a lossless codes and when there is no error in the reconstructed pixels, we have $PSNR = \infty$. Thus, we normalize the PSNR values such that the maximum PSNR is given by $PSNR_{\max} = 10 \log_{10}(I_{\max}^2) = 48.13$ dB, where $1 \leq |I_{i,j} - \hat{I}_{i,j}| \leq 255$. Note that, we chose the parameter $R_1 = 1.6$ as it was found to be the best one to attain low Bit Error Ratio (BER) performance in [11].

The PSNR versus E_b/N_0 performance of the proposed 16HM-based TTCHM-VLC-assisted context aware when communicating over uncorrelated Rayleigh channel is depicted in Fig. 4, where the iteration number represents the iteration between VLC and TTCM decoders. Note that, the iteration number inside the TTCM decoder equals to 8. We use a 16HM-based TTCM-VLC non-cooperative scheme as our benchmark, which is denoted in the Fig. 4 as “TTCM-VLC”. Furthermore, the RN is assumed to be in the mid way between the SN and DN for our TTCM-VLC based cooperative

scheme, denoted as “TTCHM-VLC”. Observe in Fig. 4, the proposed cooperative scheme requires only approximately $E_b/N_0 = 6.25$ dB to approach the asymptotic(error-free) PSNR after the fourth iteration. However, the schemes with double iterations and single iteration require 0.25 dB and one dB more to approach a similar performance, respectively.

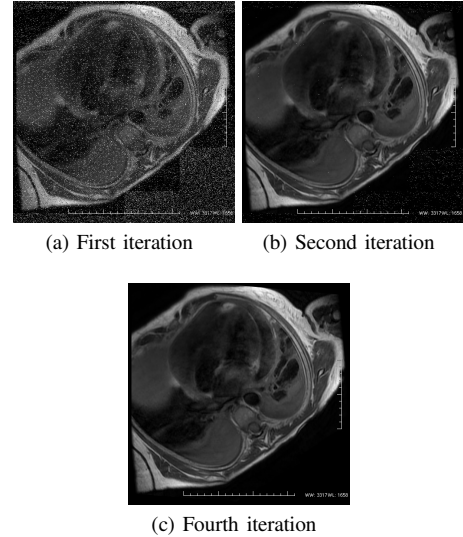
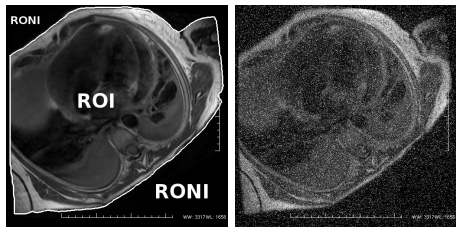


Fig. 5: Subjective image quality of an MRI medical image for the proposed 16HM-based VLC-TTCHM-assisted cooperative communication when $R_1 = 1.6$, and $E_b/N_0 = 6.25$ dB and the number of iteration between TTCM and VLC decoders are (from left) one, two, and four, respectively. Note that both phases links are subject to uncorrelated Rayleigh fading channel.

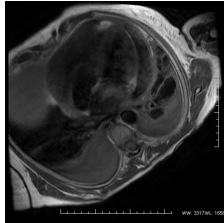
The subjective image quality results in Fig. 5 illustrate the effect of the iteration number on the reconstructed images. Hence, the image after four iteration appears to be perfect as shown in Fig. 5c, while few artefacts in ROI can be seen in Fig. 5b where the iteration number has been reduced to two. However, the single iteration based image is hard to diagnose as seen in Fig. 5a. Observe in Fig. 5b that, the use of the RN for transmission has enhanced the reception quality of the ROI area, thus this would improve the diagnosis further. As expected the proposed cooperative scheme outperforms the non-cooperative “TTCM-VLC” benchmark by $9.5 - 7.0 = 2.5$ dB, $9.2 - 6.5 = 2.7$ dB and $8.4 - 6.2 = 2.2$ dB for one, two and four iterations, respectively at a PSNR = 46 dB. In line with the PSNR results, subjective image quality outputs in Fig. 6b and Fig. 6c illustrate the image quality improvements due to the employment of the RN.

IV. CONCLUSIONS

In this paper we have proposed an optimised end-to-end image codec aided TTCHM-VLC assisted cooperative communication system for transmitting telemedicine images. We amalgamated a lossless source encoder, VLC, with TTCM aided HM scheme as the SN, where we exploit this at the RN through joint decoding. A context awareness technique was used to improve the quality of the ROI, which is more vital to the diagnosis process. The proposed scheme has shown a robust performance and has outperformed the benchmark of non-cooperative counterpart by 3 dB at a level of asymptotic PSNR. In our future work, we will consider the more transmission of ultrasonography video sequence.



(a) Original image. (b) $E_b/N_0=6.25$ dB without ROI.



(c) $E_b/N_0=6.25$ dB with ROI.

Fig. 6: Subjective image quality of an MRI medical image for: a) Original image which is used here to illustrate the ROI and RONI areas (manually selection). b) The benchmark of non-ROI coding 16HM-based TTCHM-VLC direct transmission. c) The proposed scheme of 16HM-based TTCHM-VLC-assisted cooperative communication. Note in both (b) and (c) $R_1 = 1.6$, also **Four** iteration is used between the TTCM and VLC decoder, while uncorrelated Rayleigh fading channel is used.

REFERENCES

- [1] R. S. H. Istepanian, N. Philip, and M. Martini, "Medical QoS provision based on reinforcement learning in ultrasound streaming over 3.5G wireless systems," *IEEE J. Sel. Areas Commun.*, vol. 27, no. 4, pp. 566–574, 2009.
- [2] R. S. H. Istepanian, N. Philip, M. Martini, N. Amso, and P. Shorvon, "Subjective and objective quality assessment in wireless teleultrasonography imaging," in *30th Annual International Conference of the IEEE Engineering in Medicine and Biology Society, EMBS 2008.*, pp. 5346–5349, 2008.
- [3] C. Doukas and I. Maglogiannis, "Adaptive transmission of medical image and video using scalable coding and context-aware wireless medical networks," *EURASIP J. Wirel. Commun. Netw.*, vol. 2008, pp. 25:1–25:12, Jan. 2008.
- [4] M. G. Martini and C. T. E. R. Hewage, "Flexible macroblock ordering for context-aware ultrasound video transmission over mobile wimax," *Int. J. Telemedicine Appl.*, vol. 2010, pp. 6:1–6:7, Jan. 2010.
- [5] P. Robertson and T. Wörz, "Bandwidth-efficient turbo trellis-coded modulation using punctured component codes," *IEEE J. Sel. Areas Commun.*, vol. 16, pp. 206–218, Feb. 1998.
- [6] S. X. Ng, O. Alamri, Y. Li, J. Kliewer and L. Hanzo, "Near-capacity turbo trellis coded modulation design based on EXIT charts and union bounds," *IEEE Trans. Commun.*, vol. 56, pp. 2030–2039, Dec. 2008.
- [7] R. Kim and Y. Y. Kim, "Symbol-level random network coded cooperation with hierarchical modulation in relay communication," *IEEE Trans. Consumer Electron.*, vol. 55, no. 3, pp. 1280–1285, 2009.
- [8] J. Hossain, M.-S. Alouini, and V. Bhargava, "Rate adaptive hierarchical modulation-assisted two-user opportunistic scheduling," *IEEE Trans Wireless Commun.*, vol. 6, no. 6, pp. 2076–2085, 2007.
- [9] C. Hausl and J. Hagenauer, "Relay communication with hierarchical modulation," *IEEE Commun. Lett.*, vol. 11, no. 1, pp. 64–66, 2007.
- [10] Z. Li, M. Peng, and W. Wang, "Hierarchical modulated channel and network coding scheme in the multiple-access relay system," in *Communication Technology (ICCT), 2011 IEEE 13th International Conference on*, pp. 984–988, 2011.
- [11] H. Sun, Y. Shen, S.X. Ng and L. Hanzo, "Turbo Trellis Coded Hierarchical Modulation for Cooperative Communications," in *Proc. IEEE Wireless Communications and Networking Conf.*, April. 2012.
- [12] C. E. Shannon, "A mathematical theory of Communication," *The Bell system technical journal*, vol. 27, pp. 379–423, July 1948.
- [13] S. X. Ng, F. Guo, J. Wang, L.-L. Yang and L. Hanzo, "Joint source-coding, channel-coding and modulation schemes for AWGN and Rayleigh fading channels," *Electron. Lett.*, vol. 39, pp. 1259–1261, Aug. 2003.
- [14] S. X. Ng, K. Zhu and L. Hanzo, "Distributed source-coding, channel-coding and modulation for cooperative communications," in *Proc. IEEE Vehicular Technology Conf.*, (Ottawa, Canada), pp. 1–5, 6–9 Sept. 2010.
- [15] A. J. Aljohani, S. X. Ng, R. G. Maunder and L. Hanzo, "EXIT-chart aided joint source-coding, channel-coding and modulation design for two-way relaying," *IEEE Trans. Vehicular Technol.* (to be published.), 2013.
- [16] H. Ochiai, P. Mitran and V. Tarokh, "Design and analysis of collaborative diversity protocols for wireless sensor networks," in *Proc. IEEE Vehicular Technology Conf.*, (Los Angeles, USA), pp. 4645–4649, 26–29 Sept. 2004.
- [17] S. X. Ng, F. Guo, J. Wang, L.-L. Yang and L. Hanzo, "Jointly optimised iterative source-coding, channel-coding and modulation for transmission over wireless channels," in *Proc. IEEE Vehicular Technology Conf.*, (Milan, Italy), pp. 313–317, 17–19 May 2004.
- [18] R. G. Maunder, J. Wang, S. X. Ng and L. Hanzo, "On the performance and complexity of irregular variable length codes for near-capacity joint source and channel coding," *IEEE Trans. Wireless Commun.*, vol. 7, pp. 1338–1347, April 2008.
- [19] L. Hanzo, R. G. Maunder, J. Wang and L.-L. Yang, *Near-Capacity Variable-Length Coding: Regular and EXIT-Chart-Aided Irregular Designs*. Wiley-IEEE Press, 2010.
- [20] Y. Takishima, M. Wada and H. Murakami, "Reversible variable length codes," *IEEE Trans. Commun.*, vol. 43, no. 234, pp. 158–162, 1995.